Journal of Solid State Chemistry **149,** 333–337 (2000)
doi:10.1006/jssc.1999.8536, available online at http://www.idealibrary.com on IDEAL®

Phase Relations of the SrO–Ho_2O_3–CuO_x System

W. Wong-Ng, J. Dillingham, and L. P. Cook

Ceramics Division, National Institute of Standards and Technology, Gaithersburg, Maryland 20899

Received March 31, 1999; in revised form October 7, 1999; accepted October 22, 1999

The phase diagram of the SrO–R_2O_3–CuO_x system, where R = Ho, was investigated in air. The tie-line relationships of the system were determined. The Sr analog of the high T_c superconductor $Ba_2HoCu_3O_{6+x}$ was not observed in this system. Two ternary phases were found, namely, the "14–24" solid solution $Sr_{14-x}Ho_xCu_{24}O_{41}$ and the "green phase" $SrHo_2CuO_5$. Holmium was found to substitute for the Sr site in the solid solution $Sr_{14-x}Ho_xCu_{24}O_{41}$ up to the value of $x \approx 5$. The melting temperature range of this solid solution is from 975 to 1025°C, for $x = 0$ to $x = 5$, respectively. The green phase is isostructural to its Ba analog, $BaHo_2CuO_5$, and is orthorhombic with space group *Pbnm* and cell parameters $a = 7.0971(13)$ Å, $b = 12.0262(23)$ Å, and $c = 5.5849(12)$ Å. A comparison of the Ho system with reported systems of R = La, Nd, and Y indicated that a trend exists. The larger the lanthanide ions, the more complicated the phase diagrams, i.e., with a greater number of ternary phases/solid solutions. Despite similar ionic radii between Ho^{3+} and Y^{3+}, the phase diagrams of these two systems are rather different. The green phase $SrHo_2CuO_5$ is not stable in the Y system.

INTRODUCTION

Due to the presence of high-temperature superconductors such as $Ba_2RCu_3O_{6+x}$, $Ba_2RCu_4O_x$, and $Ba_4R_2Cu_7O_x$, a great deal of phase equilibrium research effort were conducted on the BaO–R_2O_3–CuO_x systems (R = lanthanides and Y) in the past decade (1, 2). Further insights regarding the crystal chemistry and phase equilibria of the high T_c phases may be provided by the study of Ba/Sr substitution. Among the Sr–R–Cu–O systems, the members with R = La (3), Nd (4), and Y (5, 6) were reported. Although the analogs of the high T_c phases were not found in these Sr systems, the Sr-doped $Sr_{14}Cu_{24}O_{41}$ phase was reported to have interesting properties, such as anomalous microwave and magnetic properties (7–9), and it can also become superconducting under high pressure (10).

The primary goal of this project was to investigate the subsolidus relations of the SrO–Ho_2O_3–CuO_x system and to compare the phase diagram of the Ho system with known SrO–R_2O_3–CuO_x analogs.

EXPERIMENTAL[1]

Conventional solid state sintering techniques were employed for sample preparation in the SrO–R_2O_3–CuO_x system. A total of 38 compositions were prepared for this study. Well-mixed stoichiometric powders of $SrCO_3$, Ho_2O_3, and CuO were compacted by pressing the powder in a pelletizing die to about 0.3 GPa. The compacted powders were heat-treated in air at 750, 850, and 930°C for a total of 5–7 days. Each time after the samples were taken out of the furnace, they were reground and repelletized.

X-ray powder diffraction was used to identify the phase assemblages and to confirm the solid solution range and phase purity of single phases. A computer-controlled automated diffractometer equipped with a θ-compensation slit and Cu$K\alpha$ radiation was operated at 45 kV and 40 mA. The radiation was detected by a scintillation counter and a solid state amplifier. The Siemens software package and the reference X-ray diffraction patterns of the ICDD Powder Diffraction File (PDF) (11) were used for phase identification. Lattice parameter determination of selected phases was achieved using the locally modified NBSLSQ least-squares refinement program (12).

The melting study of the ternary oxides was conducted using differential thermal analysis/thermal gravimetric analysis (DTA/TGA). Simultaneous DTA/TGA experiments were performed using a Mettler TA-1 thermoanalyzer. Samples were placed in high-density MgO crucibles, and an α-alumina reference was used. The system was calibrated against the melting point of Au (1063°C). The DTA/TGA system was arranged to allow a fresh flow of purified air (with CO_2 and moisture removed) past the sample during analysis. Event temperatures were estimated to have standard uncertainties of <10°C. A heating rate of 4°C/min was used. Temperatures of the melting events were selected on the basis of the first heating cycle.

[1] The purpose of identifying the equipment in this article is to specify the experimental procedure. Such identification does not imply recommendation or endorsement by the National Institute of Standards and Technology.

0022-4596/00

RESULTS AND DISCUSSION

From results of powder X-ray diffraction of the 33 samples, the phase equilibrium diagram of the SrO–Ho_2O_3–CuO_x system was constructed (Fig. 1). This phase diagram is discussed systematically below in terms of the crystallography and crystal chemistry of the binary and ternary compounds and also the tie-line relationships of the binary and ternary compounds involved. The compounds of the binary systems have been reported in literature and will be discussed first.

(1) SrO–CuO_x

The phase diagram of the SrO–CuO_x system was reported by Liang *et al.* (13) and Suzuki *et al.* (14). There compounds were reported, namely, Sr_2CuO_3, $SrCuO_2$, and $Sr_{14}Cu_{24}O_{41}$ (commonly known as the 14–24 phase).

The Sr_2CuO_3 phase is orthorhombic (*Immm*), with lattice parameter $\mathbf{a} = 12.84$ Å, $\mathbf{b} = 3.9064$ Å, and $\mathbf{c} = 3.4957$ Å (PDF 34-283) (11). Holmium was not found to substitute for strontium. Hiroi *et al.* (15) reported that Sr_2CuO_3 can be oxidized to form tetragonal Sr_2CuO_{3+x} using a belt-type apparatus under high oxygen pressure of 600 bar of O_2 (775 °C). A tetragonal supercell of $\mathbf{a} = 21.323$ Å ($4\sqrt{2}\mathbf{a}'$, $\mathbf{a}' = 3.7695(7)$ Å) and $\mathbf{c} = 12.529(2)$ Å was given in PDF 47-487 (11).

The $SrCuO_2$ phase is orthorhombic (*Amam*), with lattice parameters $\mathbf{a} = 3.9136(2)$ Å, $\mathbf{b} = 16.3313(8)$ Å, and $\mathbf{c} = 3.5730(2)$ Å (PDF 39-1492). Similar to Sr_2CuO_3, solid solution formation with Ho was not found. Under high-pressure conditions (i.e., 775°C and 350 bar of O_2), nonstoichiometric $Sr_{0.74}CuO_2$ can be formed (16) (PDF 47-486). Under Ar at 920°C, a reduced phase $SrCu_2O_2$ was reported (17).

Hiroi *et al.* (18) further indicated that using a belt-type apparatus under high pressure and high temperature, $Sr_2Cu_3O_{5+x}$ can be prepared. The $Sr_2Cu_3O_5$ phase was found to be orthorhombic (*Cmmm*), and $\mathbf{a} = 3.9297(2)$ Å, $\mathbf{b} = 19.399(1)$ Å, and $\mathbf{c} = 3.4588(2)$ Å (PDF 47-1677).

The $Sr_{14}Cu_{24}O_{41}$ phase was first studied by Roth *et al.* (19) (PDF 39-489). The structure of this phase is rather complicated and was determined by both Siegrist *et al.* (20) and McCarron *et al.* (21). According to Siegrist *et al.* (20) $Sr_{14}Cu_{24}O_{41}$ has an orthorhombic *F*-centered subcell with a dimension of $\mathbf{a} = 11.3$ Å, $\mathbf{b} = 13.0$ Å, and $\mathbf{c} = 3.9$ Å; and the superstructure consists of a **c** axis of a 7-fold increase ($\mathbf{c} = 27.3$ Å), giving rise to a space group of *Cccm*. The structure basically consists of Cu–O planes (pyramids) and linear Cu–O chains. McCarron *et al.* (21), however, considered the structure of $Sr_{14}Cu_{24}O_{41}$ from a different point of view. They determined the structure to consist of two unique subcells, leading to an overall space group of *Pcc*2. The structure is best described as two interpenetrating structures: one with Sr–(Cu_2O_3 sheets)–Sr layers in an orthorhombic cell, and a second structure with layers of CuO_2 chains in a cell with identical lattice parameters **a** (11.459 Å) and **b** (13.368 Å), but the **c** value is much different (2.749 Å as compared to 3.931 Å). These two subcells are nearly commensurate at 7-fold **c** (sheet, of 27.372 Å) and 10-fold **c**′ (chain, of 27.534 Å).

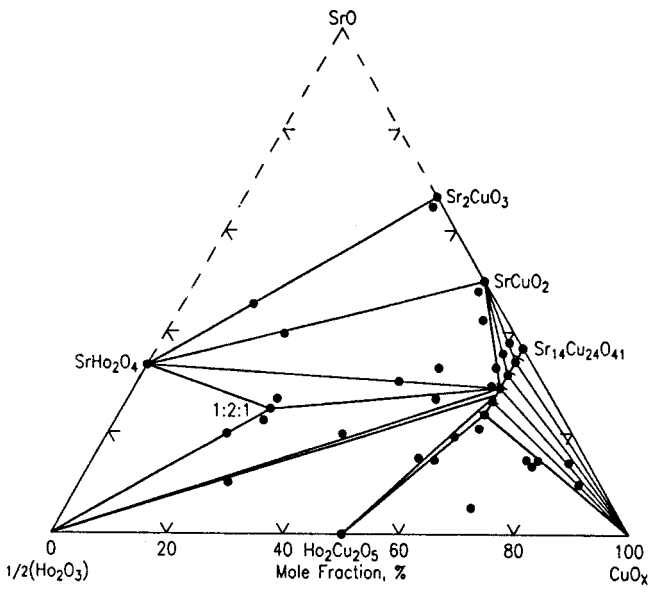

FIG. 1. Phase diagram of the SrO–$\frac{1}{2}Ho_2O_3$–CuO_x system in air at 930°C. Samples compositions are indicated as filled circles. The dashed lines were used to indicate area not extensively investigated in this study.

(2) SrO–Ho_2O_3

In this system, only one compound was found, namely, $SrHo_2O_4$ which is orthorhombic and crystallized in the space group *Pnam*, $\mathbf{a} = 10.0753(5)$ Å, $\mathbf{b} = 11.9185(5)$ Å, and $\mathbf{c} = 3.4109(3)$ Å (PDF 46-0131) (11). This phase is isostructural to that of BaY_2O_4 (22).

(3) Ho_2O_3–CuO_x

In this binary system, again only one compound, $Ho_2Cu_2O_5$, was found. $Ho_2Cu_2O_5$ is orthorhombic, $Pna2_1$, $\mathbf{a} = 10.806$ Å, $\mathbf{b} = 3.4950$ Å, and $\mathbf{c} = 12.470$ Å (PDF 33-458) (11). Zhang *et al.* (23) reported the presence of the Ho_2CuO_4 phase in the Ho_2O_3–CuO_x system, but it was not found in our study. Okada *et al.* (24) indicated that Ho_2CuO_4 can only be prepared under high pressure (i.e., 6 MPa pressure at 950°C). Furthermore, from various previous studies (25, 26), it was concluded that, under ambient conditions, the R_2CuO_4 phases can form in the R_2O_3–CuO_x system with larger R (R = La, Nd, Sm, Eu, Gd). With smaller R (R = Dy, Ho, Er, Tm, Yb, Lu), $R_2Cu_2O_5$ phases form instead of R_2CuO_4.

(4) SrO–$\frac{1}{2}Ho_2O_3$–CuO_x

There are only two ternary oxides in this system, namely, $SrHo_2CuO_5$ and the solid solution $Sr_{14-x}Ho_xCu_{24}O_{41}$. The Sr analog of the high T_c $Ba_2YCu_3O_7$-type phase did not form. It was reported that such a phase can only be formed under high pressure (27–29).

(a) Solid solution of $Sr_{14-x}Ho_xCu_{24}O_{41}$ (the 14–24 phase). X-ray diffraction patterns of the selected solid solution members of $Sr_{14-x}Ho_xCu_{24}O_{41}$ is shown in Fig. 2. The similarity of the patterns and the displacements of corresponding peaks toward higher 2θ values as Sr^{2+} is substituted by the smaller Ho^{3+} illustrated. The solid solution range (x) appears to cover a value of $0 < x < 5$. In general, among the 14–24 lanthanide analogs, it is expected that the closer match of the ionic radius of the R^{3+} with Sr^{2+}, the greater the solid solution extent; however, it was found that the extent of this solid solution varies among the reported systems. For example, while the x value was reported to be "5" in the Y analogs and larger in the Nd analog ($x \approx 7$) (5), as expected, it was reported to be of a small value of "4" for the La system. In the Ca-substituted compound $Sr_{14-x}Ca_xCu_{24}O_{41}$, x was also found to be as high as "7" (19) and "8" (14).

According to Siegrist *et al.* (20), the substituted $A_{14-x}A'_xCu_{24}O_{41}$ phase also has an F-centered orthorhombic subcell and a *Cccm* supercell. Despite that fact that there are four available crystallographic sites of Sr, there appears to be no site preference between divalent and trivalent ions of various sizes.

DTA results show that the initial melting temperature of the $Sr_{14-x}Ho_xCu_{24}O_{41}$ series increases from 975°C (30) to 1005, 1010, 1020, 1022, and 1025°C as x increases from 0 to 5. Therefore, the melting temperature of $Sr_{14-x}Ho_xCu_{24}O_{41}$ is best described as a range of $\approx$ 975–1025°C.

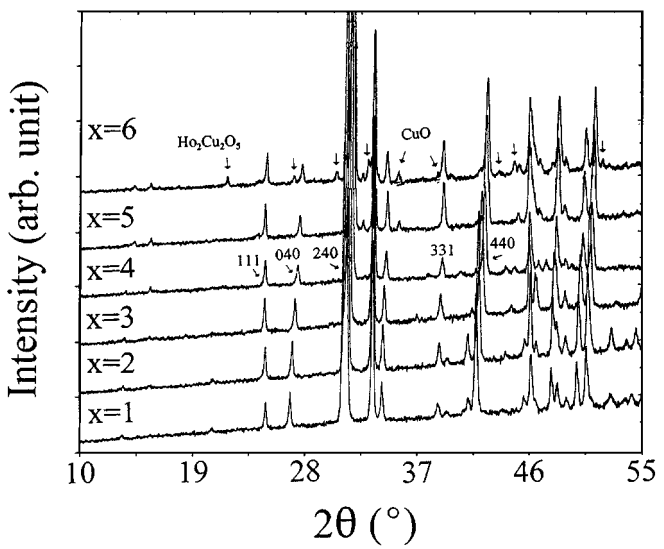

FIG. 2. X-ray diffraction patterns of the solid solution $(Sr_{1-x}Ho_x)_{14}Cu_{24}O_{41}$. At $x > 5$, significant amounts of CuO and Ho_2CuO_4 are also evident.

(b) The $SrHo_2CuO_5$ phase. The $SrHo_2CuO_5$ phase is green, and the X-ray diffraction pattern is rather similar to the green-phase analog of $BaHo_2CuO_5$ (31, 32), which crystallizes in the space group of *Pbnm*. Least-squares refinement gives the approximate lattice parameter of this phase to be $\mathbf{a} = 7.0971(13)$ Å, $\mathbf{b} = 12.0262(23)$ Å, and $\mathbf{c} = 5.5849(12)$ Å. Since X-ray patterns of $Sr_{1.1}Ho_{1.9}CuO_5$ and $Sr_{0.9}Ho_{2.1}CuO_5$ did not correspond to those of a single phase, $SrHo_2CuO_5$ did not have a significant solid solution range and is considered as a stoichiometric compound. Furthermore, it is interesting to see that despite the fact that the ionic radius (33) of Y^{3+} and Ho^{3+} are of the same value of 0.96 Å, the SrY_2CuO_5 phase does not form (5, 6). Similar to the $Sr_2RCu_3O_x$ phase, it is plausible that the SrY_2CuO_5 phase can be formed under high pressure. $SrHo_2CuO_5$ was found to melt at about 1020°C, substantially lower than the Ba analog which is well above 1200°C (34)

(c) Tie-line relationships. Phase compatabilities of the SrO–$\frac{1}{2}R_2O_3$–CuO_x system are shown in Fig. 1. Starting from the SrO corner of the SrO–$\frac{1}{2}Ho_2O_3$–CuO_x system and following down to the Ho_2O_3–CuO_x binary edge, we found the following tie-lines: $SrHo_2O_4$–Sr_2CuO_3, $SrHo_2O_4$–$SrCuO_2$, $SrHo_2O_4$–$SrHo_2CuO_5$, and Ho_2O_3–$SrHo_2CuO_5$.

The solid solution of $Sr_{14-x}Ho_xCu_{24}O_{41}$ was found to be compatible with six phases, giving rise to various tie-line bundles. The widest tie-line bundles connect the $Sr_{14-x}Ho_xCu_{24}O_{41}$ solid solution to CuO ($x = 0$–5). Additional tie-lines connect to $SrCuO_2$ ($x = 0$–2.5), to $SrHo_2O_4$ ($x = 2.5$–2.8), to $SrHo_2CuO_5$ ($x = 2.8$–3.0), to Ho_2O_3 ($x = 3$–3.5), and to $Ho_2Cu_2O_5$ ($x = 3.5$–5.0).

(5) A Comparison with the BaO–Ho_2O_3–CuO_x System

A comparison of the SrO–$\frac{1}{2}Ho_2O_3$–CuO_x diagram with the BaO–$\frac{1}{2}Ho_2O_3$–CuO_x system (1, 2, 25, 26) reveals that there are substantial differences. When the studies were conducted in air (35, 36), three ternary oxide phases were found in the Ba system, namely, the high T_c superconductor $Ba_2RCu_3O_{6+x}$ (2:1:3) phase, the often coexisting green phase $BaHo_2CuO_5$, and another perovskite solid solution 3:1:2 ss (Ba:Ho:Cu). When the samples were prepared under oxygen, two perovskite phases were identified as the 1:4:3 and 1:6:3 phases (37). In the Sr system, however, neither 2:1:3 nor 3:1:2 ss was found in air.

In the BaO–CuO_x binary system (when prepared in air), there is only one barium cuprate phase, $BaCuO_2$, but three phases were found in the SrO–CuO_x system, as discussed above.

(6) A Comparison with SrO–$\frac{1}{2}R_2O_3$–CuO_x (R = La, Nd, and Y)

The phase diagrams of the La, Nd, and Y analogs are shown in Figs. 3a–3c for comparison. Substantial differences can also be seen among these diagrams. A comparison of the SrO–$\frac{1}{2}Ho_2O_3$–CuO_x system with these systems indicates that a similar trend to that of the Ba systems (1, 2, 25) exists in the Sr systems as well. The ionic size of R^{3+} appears to be a dominant factor for determining the number of phases formed. The ionic size of Sr^{2+} is 1.21, 1.26, and 1.31 Å for VII, VIII-, and IX-coordination, respectively, and the ionic size of R^{3+} (Y^{3+} to La^{3+}) ranges from 0.96 to 1.10 Å for VII-coordination, from 1.019 to 1.160 Å for VIII-coordination, and form 1.073 to 1.216 Å for IX-coordination (33). The larger the lanthanide ions, the more complicated the phases diagrams, i.e., with a greater number of ternary phases/solid solutions, the number decreases as the size of R decreases. In the La system there are five ternary solid solution series (3), namely, $(La, Sr)_2CuO_{4-\delta}$ ($\delta > 0$),

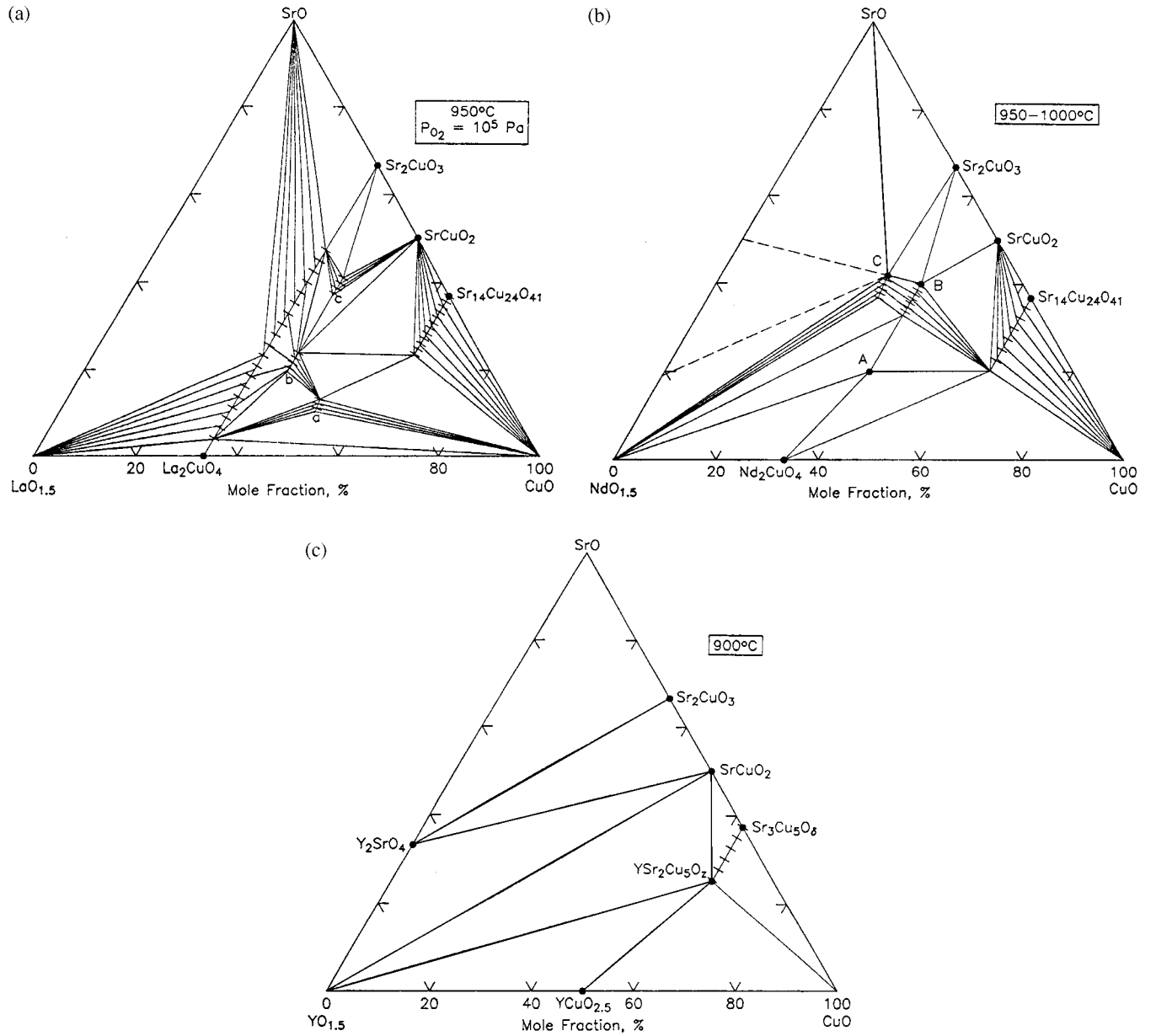

FIG. 3. Phase diagrams of the SrO–$\frac{1}{2}R_2O_3$–CuO_x systems: (a) R = La (3), (b) R = Nd (4), and (c) R = Y (5). In the La system, **a** = $La_{8-x}Sr_xCu_8O_{20-\delta}$ ($1.6 \le x \le 2.0$), **b** = $La_{2-x}Sr_{1+x}Cu_2O_{6+\delta}$ ($0.05 \le x \le 0.15$), and **c** = $La_{1+x}Sr_{2-x}Cu_2O_{5.5+\delta}$ ($0.05 \le x \le 0.15$). In the Nd system, **a** = $SrNd_2Cu_2O_6$, **b** = $Sr_{2-x}Nd_{1+x}Cu_2O_y$ ($0 \le x \le 0.4$), and **c** = $Sr_xNd_{2-x}CuO_y$ ($1.2 \le x \le 1.5$).

$La_{8-x}Sr_xCu_8O_{20-\delta}$ ($1.6 \leq x \leq 2.0$), $La_{2-x}Sr_{1+x}Cu_2O_{6+\delta}$ ($0.05 \leq x \leq 0.15$), $La_{1+x}Sr_{2-x}Cu_2O_{5.5+\delta}$ ($0.05 \leq x \leq 0.15$), and $Sr_{14-x}La_xCu_{24}O_{41}$ ($0 \leq x \leq 4$). In the Nd system, there are three solid solutions and one stoichiometric compound, namely, $Sr_{2-x}Nd_{1+x}Cu_2O_y$ ($0 \leq x \leq 0.4$), $Sr_xNd_{2-x}CuO_y$ ($1.2 \leq x \leq 1.5$), $Sr_{14-x}Nd_xCu_{24}O_{41}$ ($0 \leq x \leq 7$), and $SrNd_2Cu_2O_6$ (4). In the Ho system there is only one ternary solid solution series, $Sr_{14-x}Ho_xCu_{24}O_{41}$, $0 \leq x \leq 5$, together with a stoichiometric ternary compound $SrHo_2CuO_5$. Finally, in the Y system, only one ternary solid solution series, $Sr_{14-x}Y_xCu_{24}O_{41}$, $0 \leq x \leq 5$, is found.

ACKNOWLEDGMENTS

Partial financial support from Department of Energy of acknowledged. Ms. Evan Hayward and Mr. N. Swanson are acknowledged for their assistance in the graphic work.

REFERENCES

1. T. A. Vanderah, R. S. Roth, and H. F. McMurdie, "Phase Diagrams for High T_c Superconductors." The American Ceramic Society, Westerville, OH, 1997.
2. J. D. Whitler, and R. S. Roth, "Phase Diagrams for High T_c Superconductors." The American Ceramic Society, Westerville, OH, 1991.
3. D. M. DeLeeuw, *J. Less-Common Met.* **150,** 95–107 (1989).
4. X. L. Chen, J. K. Liang, C. Wang, G. H. Rao, X. R. Xing, Z. H. Song, and Z. Y. Qiao, *J. Alloys Compd.* **205**(1–2), 101–106 (1994).
5. Y. Ikeda, Y. Oue, K. Inaba, M. Takano, Y. Bando, Y. Takeda, R. Kanno, H. Kitaguchi, and J. Takada, *Funtai oyobi Funmatsu Yakin* **35**(3), 329–332 (1988).
6. F. Wu, S. S. Xie, Z. Chen, and J. K. Ling, *J. Mater. Sci.* **27**(11), 3082–3084 (1992).
7. M. Kato, T. Adachi, and Y. Koike, *Physica C* **265,** 107–112 (1996).
8. M. Kato, K. Shiota, S. Ikeda, Y. Maeno, T. Fujita, and Y. Koike, *Physica C* **263,** 482–485 (1996).
9. F. J. Owens, Z. Iqbal, and D. Kirven, *Physica C* **267,** 147–152 (1996).
10. M. Uehara, T. Nagata, J. Akimitsu, H. Takhashi, N. Mori, and K. Kinoshita, *J. Phys. Soc. Jpn.* **65**(9), 2764–2767 (1996).
11. PDF, Powder Diffraction File produced by ICDD, 12 Campus Blvd., Newtown Square, PA, 19073–3273.
12. D. E. Appleman and H. T. Evans, Jr. Report No. PB216188, U.S. Department of Interior, National Technical Information Service, 5285 Port Royal Rd., Springfield, VA 22151 (1973); locally modified program.
13. J. K. Liang, Z. Chen, F. Wu, and S. S. Xie, *Solid State Commun.* **75**(3), 247–252 (1990).
14. R. O. Suzuki, P. Bohac, and L. J. Gauckler, *J. Am. Ceram. Soc.* **75**(10), 2833 (1992).
15. Z. Hiroi and M. Takano, *Nature* (*London*) **364,** 315 (1993).
16. P. V. P. S. S. Sastry, A. D. Robertson, E. E. Lachowski, A. Coats, and A. R. West, *J. Mater. Chem.* **5,** 1931 (1995).
17. C. Teske and Hk. Mueller-Buschbaum, *Z. Anorg. Allg. Chem.* **379,** 113 (1970).
18. Z. Hiroi, M. Azuma, M. Tanako, and Y. Bando, *J. Solid State Chem.* **95,** 230 (1991).
19. N. M. Hwang, R. S. Roth, and C. J. Rawn, *J. Am. Ceram. Soc.* **73**(8) 2531 (1990).
20. T. Siegrist, L. F. Schneemeyer, S. A. Sunshine, J. V. Waszezak, and R. S. Roth, *Mater. Res. Bull.* **23**(10), 1429–1438 (1988).
21. E. M. McCarron, III, M. A. Subramanian, J. C. Calabrese, and R. I. Harlow, *Mater. Res. Bull.* **23**(10), 1355 (1988).
22. G. A. Costa, M. Ferretti, M. L. Fornasini, E. A. Franceschi, and G. L. Olcese, *Powder Diff.* **4,** 12 (1989).
23. Y. L. Zhang, J. K. Liang, X. R. Chen, G. H. Rao, H. B. Liu, Y. M. Ni, D. N. Zheng, and S. Xie, *J. Less-Common Met.* **146,** 121–125 (1989).
24. H. Okada, M. Takano, and M. Takeda, *Physica C* **166,** 111 (1990).
25. W. Wong-Ng, B. Paretzkin, and E. Fuller, *J. Solid State Chem.* **85,** 117–132 (1990).
26. W. Wong-Ng, and L. P. Cook, *in* "Superconducting Engineering," AICNE Symposium Series, Vol. 88, p. 11. American Chemical Engineering Society, 1992.
27. B. Dabrowski, K. Rogacki, J. W. Koenitzer, K. R. Poeppelmeier, and J. D. Jorgensen, *Physica C* **277,** 24–35 (1997).
28. B. Okai, *Jpn. J. Appl. Phys.* **29,** L2180 (1990).
29. M. R. Chandrachood, P. K. Narwnkar, D. E. Morris, and A. P. B. Sinha, *Physica C* **194,** 205 (1992).
30. W. Wong-Ng, L. P. Cook, and W. Greenwood, *Physica C* **299,** 9–14 (1998).
31. W. Wong-Ng, M. Kuchinski, B. Paretzkin, and H. F. McMurdie, *Powder Diff.* **4**(1), 2 (1989).
32. S. F. Watkins, F. R. Fronczek, K. S. Wheelock, R. G. Goodrich, W. O. Hamilton, and W. W. Johnson, *Acta Crystallogr. C* **44,** 3–6 (1988).
33. R. D. Shannon, *Acta Crystallogr. A* **32,** 751–767 (1976).
34. W. Wong-Ng and L. P. Cook, *J. Res. Natl. Inst. Stand. Technol.* **103**(4), 379–403 (1998).
35. E. Hodorowicz, S. A. Hodorowicz, C. Raymond, and H. A. Eick, *J. Solid State Chem.* **98,** 187–197 (1992).
36. S. N. Koshcheeva, V. A. Fotiev, A. A. Fotiev, and V. G. Zubkov, *Izv. Akad. Nauk SSR Neorg. Mater.* **26**(7), 1491–1494 (1990).
37. K. Osamura, and W. Zhang, *Z. Metallkd.* **84**(8), 522–528 (1993).